

Fluxes of soot black carbon to South Atlantic sediments

Rainer Lohmann,¹ Kevyn Bollinger,¹ Mark Cantwell,² Johann Feichter,³
Irene Fischer-Bruns,³ and Matthias Zabel⁴

Received 7 May 2008; revised 15 December 2008; accepted 22 December 2008; published 24 March 2009.

[1] Deep sea sediment samples from the South Atlantic Ocean were analyzed for soot black carbon (BC), total organic carbon (TOC), stable carbon isotope ratios ($\delta^{13}\text{C}$), and polycyclic aromatic hydrocarbons (PAHs). Soot BC was present at low concentrations (0.04–0.17% dry weight), but accounted for 3–35% of TOC. Fluxes of soot BC were calculated on the basis of known sedimentation rates and ranged from 0.5 to 7.8 $\mu\text{g cm}^{-2} \text{a}^{-1}$, with higher fluxes near Africa compared to South America. Values of $\delta^{13}\text{C}$ indicated a marine origin for the organic carbon but terrestrial sources for the soot BC. PAH ratios implied a pyrogenic origin for most samples and possibly a predominance of traffic emissions over wood burning off the African coast. A coupled ocean-atmosphere-aerosol-climate model was used to determine fluxes of BC from 1860 to 2000 to the South Atlantic. Model simulation and measurements both yielded higher soot BC fluxes off the African coast and lower fluxes off the South American coast; however, measured sedimentary soot BC fluxes exceeded simulated values by $\sim 1 \mu\text{g cm}^{-2} \text{a}^{-1}$ on average (within a factor of 2–4). For the sediments off the African coast, soot BC delivery from the Congo River could possibly explain the higher flux rates, but no elevated soot BC fluxes were detected in the Amazon River basin. In total, fluxes of soot BC to the South Atlantic were $\sim 480\text{--}700 \text{ Gg a}^{-1}$ in deep sea sediments. Our results suggest that attempts to construct a global mass balance of BC should include estimates of the atmospheric deposition of BC.

Citation: Lohmann, R., K. Bollinger, M. Cantwell, J. Feichter, I. Fischer-Bruns, and M. Zabel (2009), Fluxes of soot black carbon to South Atlantic sediments, *Global Biogeochem. Cycles*, 23, GB1015, doi:10.1029/2008GB003253.

1. Introduction

[2] Black carbon (BC) is a summary term for heterogeneous, aromatic and carbon-rich compounds, which are also recalcitrant in the environment [Goldberg, 1985]. Soot BC particles are formed by the condensation of small aromatic moieties in the gas phase of high-temperature combustion processes. Chars result from incomplete combustion of solid fuels, (e.g., trees, grass) for which the cellular structure of the original material remains visible. In contrast, charcoals are the solid residues of coal combustion for which the cellular structure is not visible anymore. Chars and charcoal are not as stable as soot-like BC in the environment [e.g., Elmquist *et al.*, 2006; Nguyen *et al.*, 2004].

[3] Globally, the main emission sources of BC are forest fires, biomass burning and fossil fuel utilization, mostly located in Africa and Southeast Asia [Bond *et al.*, 2004;

Cooke *et al.*, 1999]. BC plays a major role in climate change estimates through its direct and indirect effects on radiation budgets and changes in albedo [e.g., Crutzen and Andreae, 1990; Schult *et al.*, 1997]. BC fluxes are also an important part of the global carbon cycle [Kuhlbusch and Crutzen, 1995; Kuhlbusch, 1998; Seiler and Crutzen, 1980]. An “ideal” complete combustion process would release all carbon as CO_2 , and make it available for subsequent biological uptake. In reality, combustion processes are always incomplete. The burning of fossil fuels and biomass produces BC particles, and thus transforms this otherwise rapidly cycling organic carbon (OC) into BC [Bird and Cali, 1998; Seiler and Crutzen, 1980]. This process removes atmospheric carbon from the active carbon cycle, at least on short geological timescales of hundreds to thousands of years [e.g., Bird *et al.*, 1999; Kuhlbusch and Crutzen, 1995; Schmidt *et al.*, 2002]. Knowing the amount of carbon temporarily “locked away” as BC is important in our understanding of carbon fluxes, which is a key part of being able to project future climates. Many studies have focused on measuring, predicting and understanding the atmospheric emissions, presence and effects of BC particles [e.g., Bond *et al.*, 2004; Cooke *et al.*, 1999; Hansen *et al.*, 2005; Ito and Penner, 2005; Kinne *et al.*, 2003; Sato *et al.*, 2003; Seiler and Crutzen, 1980].

¹Graduate School of Oceanography, University of Rhode Island, Narragansett, Rhode Island, USA.

²ORD/NHEERL-Atlantic Ecology Division, U.S. Environmental Protection Agency, Narragansett, Rhode Island, USA.

³Max Planck Institute for Meteorology, Hamburg, Germany.

⁴MARUM Geowissenschaften, University of Bremen, Bremen, Germany.

[4] The South Atlantic Ocean is of particular interest in this regard, as it is situated in between two continents that are strongly impacted by biomass burning and natural fires [Bond *et al.*, 2004; Cooke *et al.*, 1999]. Atmospheric transport distributes these emission plumes, especially from Africa, across the South Atlantic [Crutzen and Andreae, 1990] resulting in the deposition of BC particles to the ocean basin [Cooke *et al.*, 2002]. Indeed, the long-range transport and atmospheric deposition of BC was observed in dust collected on a buoy off the coast of Africa [Eglinton *et al.*, 2002].

[5] While the emission and deposition of BC for the recent past has been examined in model studies [e.g., Stier *et al.*, 2005, 2006], only few studies have been conducted to verify these computations by actually measuring the records of these fluxes in the environment [e.g., Elmquist *et al.*, 2007]. Several studies have been presented with a high temporal resolution by analyzing carbonaceous particles in ice cores from alpine glaciers [Jenk *et al.*, 2006; Lavanchy *et al.*, 1999]. However, little work has been conducted to establish regional budgets of BC fluxes. Most marine BC research to date has been carried out in coastal environments [e.g., Cornelissen *et al.*, 2005; Gustafsson and Gschwend, 1997; Lohmann *et al.*, 2005; Mannino and Harvey, 2004], while little attention has been paid to regional or global scales. Notable exceptions are studies of soot BC fluxes on the New England coastal shelf [Gustafsson and Gschwend, 1998], the Pan-Arctic Rivers [Elmquist *et al.*, 2008], and a study looking at the importance of the Mississippi River in delivering soot BC to the Atlantic Ocean [Mitra *et al.*, 2002]. Schmidt and Noack [2000] and Kuhlbusch [1998] summarized global BC budgets and hypothesized that deep sea sediments are major sinks of BC. However, these estimates were based on an extremely limited sample size of a few sediments per ocean basin.

[6] BC displays high affinities for planar aromatic compounds, especially polycyclic aromatic hydrocarbons (PAHs) [e.g., Gustafsson and Gschwend, 1997]. During atmospheric transport, PAHs preferentially adhere to BC-like particles [Dachs and Eisenreich, 2000; Lohmann and Lammel, 2004], which could explain their observed atmospheric stability [see Lohmann and Lammel, 2004]. The association of organic tracer molecules, such as PAHs, to BC offers geochemists the possibility to infer the BC emission sources [Blumer, 1976]. In addition, stable carbon isotope ratios ($\delta^{13}\text{C}$) are characteristic of different carbon sources and can be used to trace the origin of BC, provided the signature does not change from fuel to the aerosols. Currie *et al.* [1999] concluded that aerosols from controlled burning experiments retained the $\delta^{13}\text{C}$ signature within the range of the fuel's isotope heterogeneity.

[7] For this study, we analyzed previously collected deep sea surface sediments from across the South Atlantic. Our objectives were to (1) quantify the presence of soot-like BC and PAHs in deep sea sediments and derive their fluxes; (2) interpret the PAH and $\delta^{13}\text{C}$ signatures to infer possible sources of the soot BC; (3) compare our sediment-based soot BC fluxes with those independently estimated from an aerosol-climate model; and (4) make inferences on the

importance of atmospheric deposition versus riverine discharges of soot BC for the South Atlantic.

2. Materials and Methods

2.1. Sediment Samples

[8] Available sediment samples were taken by multicorer and box corers during several expeditions which have been primarily financed by the German Research Foundation (DFG) over the last 20 years [Wagner *et al.*, 2003; Zabel *et al.*, 2003]. After recovery, sediment cores were sliced immediately and stored at 4°C until their processing at Bremen University. Subsamples were freeze-dried, ground with a mortar and stored. The top (0.5 or 1 cm) sediment layer subsamples were shipped to URI-GSO individually packaged in cold storage. These samples were analyzed at URI-GSO in a special clean laboratory, which is served by its own dedicated air handler with HEPA filters for the removal of fine particles. About 5 g dry weight sediment samples were analyzed for soot BC, total organic carbon (TOC), PAHs and $\delta^{13}\text{C}$. Sediment samples' coordinates, sampling dates, sedimentation rates, sample ages and water depths are given in Table 1.

2.2. Sedimentation Rates

[9] Previously published sedimentation rates (SR) were used to estimate the ages of the sediment surface layers (see compilation by Drs. Seiter and Zabel in World Data Center for Marine Environmental Sciences (WDC-MARE), <http://www.pangaea.de>). For locations where no age models exist, SR were approximated from adjacent locations with similar water depth [see also Middelburg *et al.*, 1997]. Accumulated sedimentation ages were calculated as the ratio of the thickness of the sampled surface sediment layer over the associated SR. Integrated sediment ages varied from mostly 20–100 years off the African coast to mostly 200–400 years off the South American coast (Table 1).

2.3. Soot BC and Stable Carbon ($\delta^{13}\text{C}$) Analysis

[10] TOC consists of BC and OC. TOC and BC are measured directly, with OC accounting for the difference (or $\text{OC} = \text{TOC} - \text{BC}$). We decided to focus on soot BC, as it is the most recalcitrant form of BC [e.g., Elmquist *et al.*, 2006; Nguyen *et al.*, 2004]. Soot BC was isolated by thermochemical oxidation at 375°C (CTO-375) following [Elmquist *et al.*, 2004; Gustafsson *et al.*, 2001; Gustafsson *et al.*, 1997]. Method CTO-375 has been shown to be a selective and reproducible method optimized to isolate soot BC [e.g., Hammes *et al.*, 2007]. Furthermore, the soot BC method was geochemically consistent in downcore records that were decoupled from OC, but follow society's fuel history [e.g., Elmquist *et al.*, 2007; Louchouart *et al.*, 2007].

[11] Sediment subsamples were dried, ground and sieved (<425 μm), and spread as a thin film in prebaked porcelain crucibles. The labile OC was removed by thermal oxidation at 375°C under airflow (Compressed Air, Airgas Inc.) for 24 h in a Barnstead Thermolyne 47,900 Furnace. Hydrochloric acid (1 M, Mallinckrodt Analytical Reagent) was added dropwise with a pipette to remove carbonates until no more bubbling was observed. The remaining carbon con-

Table 1. Sampling Date, Geographic Position (Latitude/Longitude Coordinates) Water Depth, Sedimentation Rate, and Sample Age of Selected Sediment Samples From the South Atlantic Ocean

Position	GeoB Core ^a	Sampling Date	Latitude (S/N)	Longitude (W/E)	Water Depth (m)	Sedimentation Rate ^b (cm ka ⁻¹)	Age (years)
<i>Africa</i>							
Cameroon	4903	Feb. 1998	1.90	8.17	2385	1.9	263
Off Libreville	4904	Feb. 1998	0.96	8.88	1339	n/a	50 ^c
Cameroon	4905	Mar. 1998	2.50	9.39	1328	25	20
S off Libreville	4906	Mar. 1998	-0.69	8.38	1272	n/a	50 ^c
S off Libreville	4908	Mar. 1998	-0.71	6.84	3029	3.1	160
Congo fan	4913	Mar. 1998	-5.50	11.07	1300	9.8	50
Congo fan	4914	Mar. 1998	-6.90	9.00	3977	7.5	70
S off Congo fan	4915	Mar. 1998	-7.80	11.87	1302	n/a	50 ^c
Off Angola	4917	Mar. 1998	-11.9	13.07	1299	n/a	50 ^c
<i>South America</i>							
W Argentina basin	2712	Jun. 1994	-43.7	-59.33	1228	2.5	400
W Argentina basin	2715	Jun. 1994	-43.9	-57.66	3280	2.5	400
NW Argentina basin	2814	Jul. 1994	-37.6	-39.07	4949	2.5	200
Santos plateau	2818	Jul. 1994	-30.9	-38.17	3110	2.5	200
Santos plateau	2825	Aug. 1994	-32.5	-41.43	4352	2.5	200
SW Brazil basin	3822	Mar. 1996	-27.6	-37.95	4273	2.5	400
SW Brazil basin	3825	Mar. 1996	-26.2	-36.33	4279	2.5	400
SW Brazil basin	3827	Mar. 1996	-25.0	-38.55	3842	2.5	400
N Brazil basin	3909	Mar. 1996	-3.55	-36.27	3174	3.5	286
N Brazil basin	3915	Apr. 1996	-2.28	-38.02	3127	n/a	143 ^c
Amazon fan	4401	Mar. 1997	4.79	-43.46	3396	2.2	227
Amazon fan	4404	Mar. 1997	6.06	-43.74	4397	n/a	250 ^c
Amazon fan	4405	Mar. 1997	5.91	-43.75	4300	n/a	250 ^c
Amazon fan	4408	Mar. 1997	3.67	-46.13	3466	2	250

^aGeoB is the acronym for the Department of Geosciences at Bremen University, where each sample has been assigned to a specific location, water depth, cruise, and cast. Additional information for each sample can be found by its GeoB number at Publishing Network for Geoscientific and Environmental Data (<http://www.pangaea.de>) or WDC-MARE (<http://www.wdc-mare.org>).

^bSee in WDC-MARE; n/a is not available.

^cAge was estimated on the basis of the nearest core.

stituted the soot BC fraction. TOC and soot BC were analyzed for %C and $\delta^{13}\text{C}$ on a Carlo Erba NA 1500 series II Elemental Analyzer attached to a continuous flow isotope ratio mass spectrometer (Micromass Optima) at the EPA laboratory. The method detection limit (MDL) was approximately 100 ng per sample, with the lowest soot BC samples containing at least 400 ng per sample.

[12] Differences in the relative abundance of stable carbon isotopes $^{13}\text{C}/^{12}\text{C}$ are expressed in the $\delta^{13}\text{C}$ (in ‰) notation, relative to Pee Dee Belemnite (PDB). Stable carbon ratios were calculated in terms of

$$\delta^{13}\text{C} = (R_{\text{sample}}/R_{\text{standard}} - 1)/1000, \quad (1)$$

where R_{sample} is the ratio of $^{13}\text{C}/^{12}\text{C}$ in the sample, and PDB represents the $^{13}\text{C}/^{12}\text{C}$ ratio in the C standard, R_{standard} . Methyl urea (Mallinckrodt Chemicals) and a certified reference material, dogfish (National Research Council Canada) were used as quality assurance standards.

2.4. PAH Analysis

[13] After addition of 50 μL of an internal standard solution containing deuterated PAHs (d_{10} -acenaphthene, d_{10} -phenanthrene, d_{12} -chrysene and d_{12} -perylene; 5 ng μL^{-1} in nonane), sediments were thrice extracted in a metabolic shaker using acetonitrile and hexane as described elsewhere [Hartmann *et al.*, 2004]. The resulting hexane

extracts were combined and concentrated to ~ 1 mL on a rotary evaporator and treated with copper to remove elemental sulphur. The extract was passed through an activated silica column using hexane and concentrated to ~ 30 μL . 50 μL of d_{14} -terphenyl (5 ng μL^{-1}) was added as an injection standard before analysis.

[14] Samples were analyzed for PAHs on an Agilent 6890 gas chromatograph (GC) coupled to an Agilent 5973N mass spectrometer (MS) operated in the negative electronic ionization mode. For each sample, 1 μL was injected in the splitless mode onto a Varian Factor Four VF-5MS column (30 m, internal diameter 250 μm). Column flow was constant at 2 mL min^{-1} . The temperature program was as follows: hold 60°C for 3 min, increase to 120°C at 3.5°C min^{-1} , increase to 315°C at 8°C min^{-1} , and hold for 8 min. The injection port was maintained at 300°C, and the MS transfer line at 280°C.

[15] PAHs were identified by retention time and mass in selected ion monitoring. They were quantified relative to the nearest internal standard. Quantification was accomplished through the application of a six-point calibration curve by running a series of standards containing the internal and injection standards and native compounds every 15 samples. Relative response factors were derived for each compound and used to correct the peak area for differences in ionization between analytes. Mean recoveries of the internal standards were 92% for d_{10} -acenaphthene, 97% for d_{10} -phenanthrene,

Table 2. Geographic Position (Latitude/Longitude Coordinates), Surface [TOC] and [Soot BC], Soot BC/TOC Ratio, $\delta^{13}\text{C}$ of TOC and BC Fractions, Soot BC Flux, PAH Concentrations and Ratios of Selected Sediment Samples From the South Atlantic Ocean^a

Position	Latitude (S/N)	Longitude (W/E)	TOC (% dw)	Soot BC (wt %)	Soot BC/TOC	$\delta^{13}\text{C}$ (TOC) (‰)	$\delta^{13}\text{C}$ (BC) (‰)	Soot BC Flux ($\mu\text{g cm}^{-2} \text{ a}^{-1}$)	ΣPAHs (ng g^{-1})	Me-phen/phen	Fl/Fl + Py	Retene (ng g^{-1})
<i>Africa</i>												
Cameroon	1.90	8.17	1.90	0.08	0.04	-19.68	-25.67	0.5	399	0.09	0.71	7.3
Off Libreville	0.96	8.88	2.72	0.09	0.03	-20.60	-28.93	3.2	290	0.14	0.80	7.1
Cameroon	2.50	9.39	3.50	0.11	0.03	-20.86	-24.87	7.8	374	0.22	0.77	6.5
S off Libreville	-0.69	8.38	3.72	0.11	0.03	-22.05	-26.08	3.8	611	0.22	0.81	5.1
S off Libreville	-0.71	6.84	0.94	0.11	0.12	-20.75	-25.11	1.6	119	1.51	0.84	4.9
Congo fan	-5.50	11.07	3.30	0.08	0.03	-23.10	-25.28	3.0	223	0.12	0.79	3.1
Congo fan	-6.90	9.00	2.02	0.09	0.04	-30.04	-26.09	1.7	222	0.13	0.75	0.7
S off Congo fan	-7.80	11.87	1.33	0.09	0.07	n/a	-26.38	3.1	227	0.09	0.80	1.1
Off Angola	-11.9	13.07	4.47	0.16	0.04	n/a	-24.74	6.5	768	0.17	0.83	1.4
<i>South America</i>												
W Argentina basin	-43.7	-59.33	0.25	0.04	0.18	-24.87	-27.48	1.6	94	nd	nd	nd
W Argentina basin	-43.9	-57.66	0.46	0.11	0.23	-23.95	-26.63	1.6	99	nd	nd	nd
NW Argentina basin	-37.6	-39.07	0.95	0.10	0.11	-23.01	-26.29	2.6	82	0.34	0.78	2.8
Santos plateau	-30.9	-38.17	0.78	0.10	0.12	-21.59	-23.67	1.8	8	0.14	0.75	0.0
Santos plateau	-32.5	-41.43	0.58	0.07	0.13	-20.57	-25.13	1.1	10	0.71	0.69	0.2
SW Brazil basin	-27.6	-37.95	1.01	0.08	0.08	-22.59	-25.45	0.6	34	0.22	0.77	0.2
SW Brazil basin	-26.2	-36.33	0.80	0.10	0.12	-21.41	-25.67	0.6	11	0.47	0.70	0.1
SW Brazil basin	-25.0	-38.55	0.50	0.09	0.18	-22.15	-26.28	1.0	6	0.25	0.75	0.1
N Brazil basin	-3.55	-36.27	0.49	0.17	0.34	-19.56	-23.25	1.7	3	0.27	0.82	0.0
N Brazil basin	-2.28	-38.02	0.44	0.11	0.25	-20.10	-24.34	1.7	75	0.10	0.81	0.2
Amazon fan	4.79	-43.46	0.37	0.12	0.33	-23.90	-23.40	2.0	91	0.20	0.84	1.6
Amazon fan	6.06	-43.74	0.71	0.11	0.16	-20.84	-23.72	1.5	233	0.28	0.81	2.1
Amazon fan	5.91	-43.75	0.57	0.11	0.19	-20.08	-24.17	1.5	59	0.15	0.82	0.6
Amazon fan	3.67	-46.13	0.56	0.11	0.20	-22.16	-25.82	1.7	72	0.22	0.83	1.2

^a ΣPAHs are naphthalene; 1- and 2-methylnaphthalene; biphenyl; acenaphthylene; acenaphthene; fluorene; phenanthrene; anthracene; 1-, 2-, 3-, and 9-methylphenanthrenes; fluoranthene; pyrene; retene; benz[a]anthracene; chrysene; benzo[b]fluoranthene; benzo[k]fluoranthene; benzo[e]pyrene; benzo[a]pyrene; perylene; indeno[1, 2, 3-cd]pyrene; dibenz[a, h]anthracene; and benzo[ghi]perylene. Here n/a is not available and nd is not detected.

97% for d_{12} -chrysene and 110% for d_{12} -perylene. Sediments were analyzed for 26 PAHs (Table 2). PAH concentrations in laboratory blanks ranged from 4 to 17 ng per sample, typically <10% of sediment values. The MDLs for individual PAHs were on the order of 50–100 pg per sample. Samples were not corrected for blank values.

2.5. Atmospheric Model Description

[16] Simulations were performed at the Max Planck Institute (MPI) for Meteorology for the years 1860 to 2000 with the coupled aerosol-climate model ECHAM5-OM1-HAM comprising the ECHAM5 atmospheric and OM1 oceanic general circulation model, and the microphysical aerosol module HAM. The temporal evolution of anthropogenic greenhouse gas concentrations and anthropogenic aerosol emissions were prescribed. ECHAM5 [Roekner *et al.*, 2003] is the 5th generation climate model developed at the MPI for Meteorology, evolving from the model of the European Centre for Medium-Range Weather Forecasts. The microphysical aerosol module HAM [Stier *et al.*, 2005] incorporates the dominant global aerosol components: sulfate, BC, particulate organic matter, sea salt, and mineral dust. The aerosol size distribution and mixing state are represented by the superposition of seven partially internally mixed modes. The composition of each mode is prognostic within the allowed mixing state configuration and determined by the governing microphysical processes

of coagulation, condensation, and water uptake [see Stier *et al.*, 2005; Vignati *et al.*, 2004]. BC is emitted into the internally mixed hydrophobic BC Aitken mode and transferred by microphysical aging, i.e., the coagulation with hydrophilic modes and the condensation of sulfuric acid, to internally mixed hydrophilic Aitken, accumulation, and coarse modes. Hydrophobic particles coated with at least a monolayer of sulfate are transferred to the hydrophilic mode of the same size class. For wet deposition, differentiation between the hydrophobic and hydrophilic modes is represented in the form of mode-specific semiempirical scavenging parameters, with reduced scavenging ratios for the hydrophobic modes [see Stier *et al.*, 2005].

[17] Time series of the annual mean emission fluxes for anthropogenic carbonaceous aerosols from 1860 to 2000 have been provided by Toru Nozawa *et al.* (Japanese National Institute for Environmental Studies (NIES), personal communication, 2004). The inventory includes emissions originating from biomass burning, biofuel, agricultural activity, and fossil fuels. Fuel uses are based on several databases from the Food and Agriculture Organization of the United Nations (FAO), Global Emissions Inventory Activities (GEIA), and energy statistics in each nation. It should be mentioned that even for present-day emission inventories significant uncertainties exist. They differ by as much as a factor of two for fossil fuel use [e.g., Schaap *et al.*, 2004] and are even more uncertain for biomass burning emissions. These uncertainties propagate

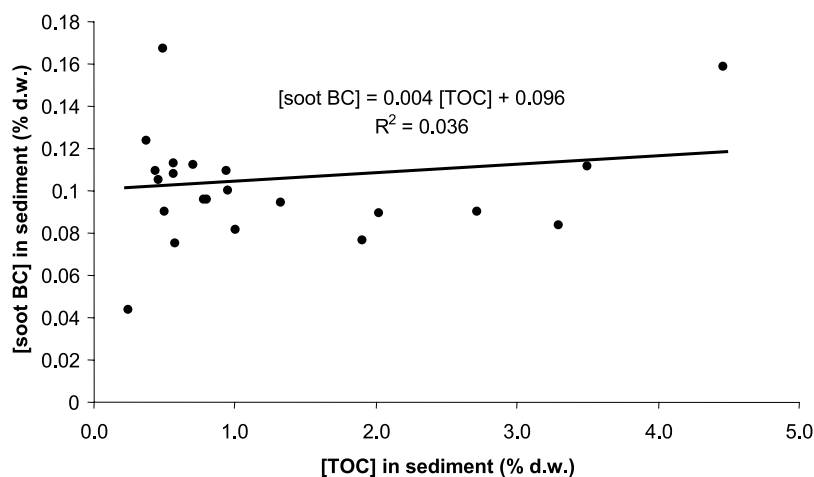


Figure 1. Soot BC concentration versus TOC concentration in South Atlantic sediments (% dw).

into past emission scenarios, and further add to uncertainties regarding economic, population, technological, and legislative developments. Further details about the emission inventory used and the model setup are given by *Stier et al.* [2006] and *Takemura et al.* [2005].

2.6. Validity of Soot BC Measurements

[18] There is ongoing discussion on the most suitable methodological approach to determining BC in the environment [e.g., *Hammes et al.*, 2007]. Following is the available evidence that our measurements gave accurate results for soot BC:

[19] 1. The soot BC concentrations are similar to those published by other groups (see below), suggesting that our numbers are reasonable.

[20] 2. *Gelinas et al.* [2001] noted that previous measurements of soot BC by method CTO-375 in sediments might have been biased because of charring of the sedimentary organic matter. This was illustrated with a graph displaying the determined soot BC fraction versus OC content, yielding increasing soot BC concentrations with increasing OC content. We have plotted the same variables, and obtained no significant correlation (Figure 1). We take this as further evidence that our measurements were not significantly affected by charring. This might be partially due to the fact that soot BC isolation was performed under a stream of air to ensure proper oxidation.

[21] 3. We analyzed both TOC and isolated soot BC for their $\delta^{13}\text{C}$ values (Table 2 and below). For most sediment samples, there was a significant difference between the $\delta^{13}\text{C}$ values of soot BC and OC, indicating again that they constitute two different pools of carbon, and that we isolated a subfraction with different properties.

[22] 4. We routinely included BC reference materials, as recommended by [*Hammes et al.*, 2007]. Our results compare well to other CTO-375 methods: $1.63\% \pm 0.13$ ($n = 4$) for urban aerosols SRM 1649a, $0.52\% \pm 0.14$ ($n = 4$) for marine sediment SRM 1941b, 0.08 and 0.13% for Vertisol and Mollisol, two soils. Blank samples (muffled sand) and false positive matrices (melanoidin, risotto char and wood char) all returned zero soot BC.

[23] 5. Finally, derived soot BC fluxes compare well with estimates based on atmospheric emission models (see next section).

3. Results and Discussion

3.1. Sedimentary Soot BC and Soot BC/TOC Ratios

[24] Soot BC was detected in all sediment samples from the South Atlantic, at concentrations ranging from 0.04 to 0.17% dry weight (dw). There was no significant difference between samples off the African or South American coasts (Table 2). Our concentrations were comparable to the few other reported concentrations of soot BC in offshore ocean sediments. For example, soot BC accounted for ~ 0.05 – 0.16% dw in sediments from the Iberian margin in the Atlantic [*Middelburg et al.*, 1999], and ~ 0.01 – $<0.2\%$ dw in Pan-Arctic river sediments [*Elmqvist et al.*, 2008] and sediments from the Gulf of Maine [*Gustafsson and Gschwend*, 1998].

[25] Soot BC/TOC ratios were calculated for the South Atlantic sediments, and ranged from 0.03 to 0.34 (Table 2). Relatively low soot BC/TOC ratios were determined in African margin sediments, with soot BC accounting for an average of 0.05 ± 0.03 ($n = 9$; range of 0.03–0.12). In fact, with two exceptions, all samples had soot BC/TOC ratios of 0.03–0.04. In contrast, sediments in the western South Atlantic were characterized by higher soot BC/TOC ratios (average: 0.19 ± 0.08 , $n = 14$; range of 0.07–0.34). The Santos plateau and the southwestern Brazil basin were characterized by relatively low soot BC/TOC ratios of 0.08–0.18. Soot BC/TOC ratios >0.20 were derived for the northern Brazil basin, in parts of the Amazon fan and in the West Argentine basin (Table 2). The Amazon fan has been termed a “sedimentary incinerator” [*Aller and Blair*, 2006], because of its high remineralization of OC, supporting our elevated soot BC/TOC ratios in those sediments.

[26] Soot BC/TOC ratios are the result of two independent processes, the fluxes of soot BC and OC (both terrestrial and marine) to the sediments and the remineralisation fluxes removing C from the sediments [e.g., *Burdige*, 2005]. The elevated fraction of soot BC off the South American coast could be explained by the generally lower sedimentation

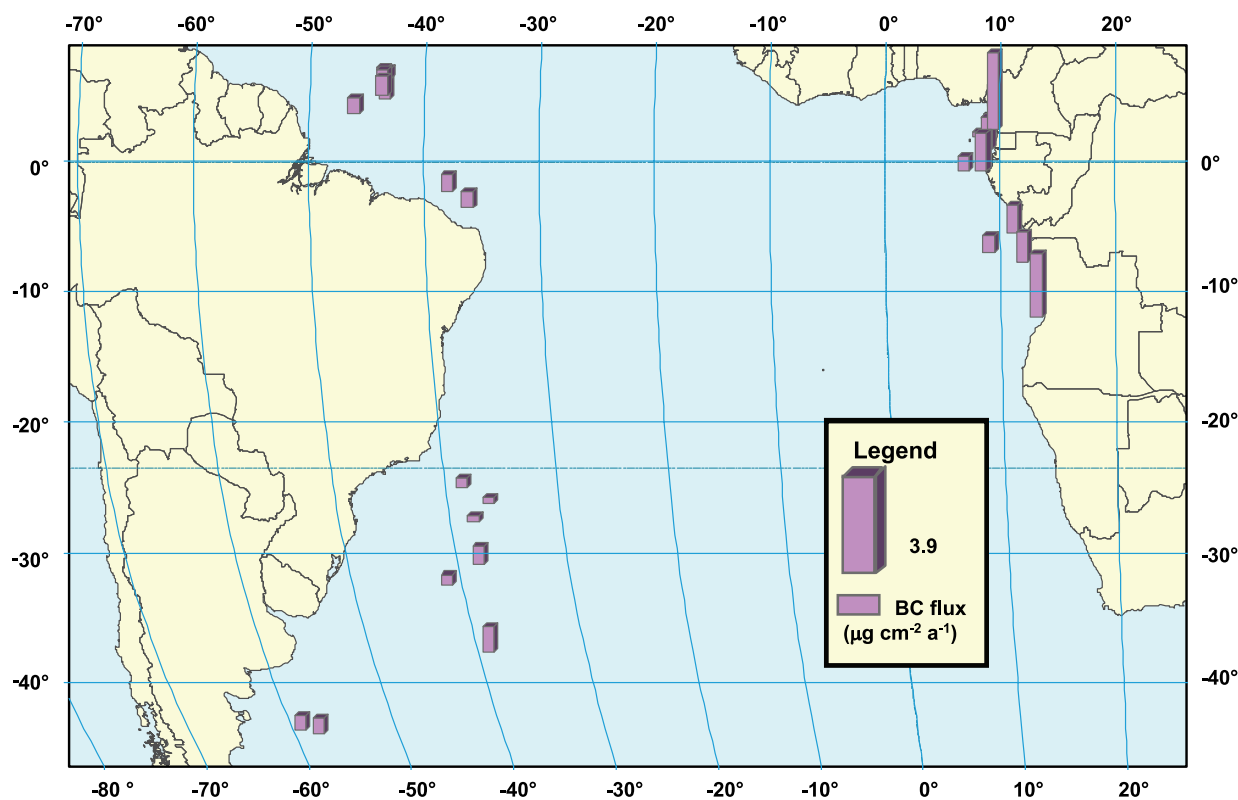


Figure 2. Derived soot BC fluxes for sediments off southwest Africa and off South America ($\mu\text{g cm}^{-2} \text{a}^{-1}$).

rates compared to locations sampled in the eastern South Atlantic. Most sediment samples analyzed off Africa had an age of less than 50 years, but an age of approximately 200 years and more off South America (Table 1). A slower sedimentation rate means that fewer solids are efficiently buried over time [e.g., Hartnett *et al.*, 1998]. This tends to enrich the more recalcitrant fractions of the carbon spectrum (e.g., soot BC). The soot BC/TOC ratios imply that soot BC is indeed rather refractory in deep sea sediments [e.g., Burdige, 2005; Middelburg *et al.*, 1999]. In these deep sea surface sediment with $\leq 1\%$ TOC, soot BC accounted for about 10–35% of TOC (Table 2).

3.2. Flux Estimates of Soot BC to the South Atlantic Ocean

[27] Soot BC accumulation rates were calculated on the basis of measured dry bulk sediment densities (of the top 3 cm), the known height of the sample analyzed and its sediment age. Fluxes varied from ~ 0.5 – $7.8 \mu\text{g cm}^{-2} \text{a}^{-1}$ (Table 2). Highest fluxes were calculated for locations in the eastern South Atlantic (on average $3.5 \pm 2.4 \mu\text{g cm}^{-2} \text{a}^{-1}$). In the western South Atlantic, soot BC fluxes were significantly lower, presumably because they were dominated by atmospheric deposition from Africa, some 6,000 km to the East (on average $1.5 \pm 0.5 \mu\text{g cm}^{-2} \text{a}^{-1}$; Table 2 and Figure 2). On the African side, soot BC fluxes were highly variable. Highest fluxes ($>6 \mu\text{g cm}^{-2} \text{a}^{-1}$) were off Cameroon and Angola, but only 2 – $3 \mu\text{g cm}^{-2} \text{a}^{-1}$ in the

Congo River fan. On the South American side, soot BC fluxes $>1.5 \mu\text{g cm}^{-2} \text{a}^{-1}$ were derived for the western Argentine basin, the northern Brazil basin and the Amazon fan. Lowest soot BC fluxes were obtained for the south-western Brazil basin (0.6 – $1.0 \mu\text{g cm}^{-2} \text{a}^{-1}$).

[28] The soot BC fluxes derived here for offshore South Atlantic sediments turned out to be much lower than fluxes reported previously for water bodies which were more impacted by anthropogenic emissions. For example, soot BC fluxes of ~ 90 – $190 \mu\text{g cm}^{-2} \text{a}^{-1}$ were estimated for the Gulf of Maine [Gustafsson and Gschwend, 1998]. Soot BC fluxes of $23 \mu\text{g cm}^{-2} \text{a}^{-1}$ and $890 \mu\text{g cm}^{-2} \text{a}^{-1}$ were reported for Lake Superior and Lake Erie, respectively [Buckley *et al.*, 2004]. In contrast, [Smith *et al.*, 1973] reported total BC fluxes of 0.01 – $0.1 \mu\text{g cm}^{-2} \text{a}^{-1}$ in preindustrial Pacific deep sea sediments. These comparisons suggest that our derived fluxes are of the right order of magnitude, substantially above preindustrial fluxes of soot BC, but well below fluxes in water bodies closer to major anthropogenic emissions. So far, we have focused on soot BC abundance and fluxes, but have not addressed what the possible sources of the soot BC could have been. The samples were therefore analyzed for their isotopic and molecular signals to decipher the sources of soot BC.

3.3. Stable Carbon Isotope Values ($\delta^{13}\text{C}$) of Soot BC and OC

[29] The isolated soot BC fractions and TOC samples were analyzed for $\delta^{13}\text{C}$ ratios. $\delta^{13}\text{C}$ values for OC were

calculated on the basis of a linear two end-member equation, in which $[OC] = [TOC] - [soot\ BC]$

$$\delta^{13}C_{OC} = (\delta^{13}C_{TOC}[TOC] - \delta^{13}C_{BC}[soot\ BC])/[OC]. \quad (2)$$

Typical $\delta^{13}C$ for marine phytoplankton are around -19% (-18 to -22%) [Holtvoeth *et al.*, 2003]. C_3 plants average $\sim -26\%$ (-23 to -28%), while C_4 plants display average $\delta^{13}C$ values of $\sim -13\%$ (-12 to -16%) [Farquhar *et al.*, 1989]. As fossil fuels are the by-products of organic material, they are depleted in ^{13}C similar to C_3 plants (around -26%) [Farquhar *et al.*, 1989]. Although there were subtle differences between the $\delta^{13}C$ values, they did not unequivocally separate the eastern from the western sedimentary carbon pools. Off Africa, the $\delta^{13}C$ of soot BC in all but one of the sediments was within -24.5 to -26.5% , consistent with the burning of C_3 plants. A similar range of $\delta^{13}C$ values was observed for aerosols originating from African biomass burning [Cachier, 1989]. In contrast, $\delta^{13}C$ values of the OC pool were mostly around -19 to -22% , similar to phytoplankton. Only the two OC fractions from the Congo River fan displayed $\delta^{13}C$ values of -23 and -30% , suggesting at least a partial terrestrial origin for the OC present in these sediments, as would have been expected.

[30] On the South American side, $\delta^{13}C$ values of the soot BC were around -23 to -26% , while $\delta^{13}C$ values of the OC varied from -18 to -24% , with most values around -18 to 21% . Samples from the Argentine basin were characterized by the lightest $\delta^{13}C$ values of -26 to -27% for soot BC, and -22 to -24% for OC, indicating a strong terrestrial influence in the sediment. Sediments from the Santos plateau and the Brazil basin displayed typical marine $\delta^{13}C$ values for the OC fraction (-18 to -22%), while the soot BC values (-23 to -26%) were consistent with a terrestrial origin. These OC and soot BC values were also measured in samples from the Amazon fan, although there was one sample each with distinctly lighter OC (-24%) and soot BC (-26%) values.

[31] These results also clearly demonstrated that the isolated soot BC fraction was fundamentally different from the surrounding OC, hence charring did not affect our results as discussed previously (see also Figure 1). Most OC samples reflected a marine origin, with the exception of samples from the Congo River fan, and a few samples off South America, which showed some evidence of terrestrial origin. The $\delta^{13}C$ values of the soot BC measured in the South Atlantic were consistent with a major terrestrial carbon source, but could not discriminate between biomass burning and fossil fuel use. Analysis of PAHs and diagnostic ratios were used to further characterize the emission sources of the soot BC.

3.4. Molecular Evidence for the Origin of Sedimentary Soot BC

[32] Total PAH concentrations varied greatly, from a few $ng\ g^{-1}$ in the deep sea sediments off the South American coast to $100s\ ng\ g^{-1}$ near the African coast (Table 2). Higher PAH concentrations off the African coast were expected in view of the prevailing wind regimes delivering

emission plumes from the African continent westward, and additional riverine discharges. Highest PAH concentrations were obtained in samples from the Congo River fan on the African side ($770\ ng\ g^{-1}$), and from the Amazon fan on the South American side ($230\ ng\ g^{-1}$), suggesting riverine inputs of PAHs.

[33] Dominant PAHs were phenanthrene (47%), followed by methylphenanthrenes (17%) and fluoranthene (5%). PAHs in a series of Pacific deep sea sediments, presumably from atmospheric long-range transport [e.g., Jaward *et al.*, 2004; Nizzetto *et al.*, 2008], were dominated by phenanthrene, followed by benzofluoranthenes and perylene [Ohkouchi *et al.*, 1999].

[34] More information about the origin of the soot BC and associated PAHs was gained by deciphering their molecular signature [Yunker *et al.*, 2002]. The methylphenanthrenes/phenanthrene ratios ($\Sigma Me\text{-phen/phen}$) were calculated for the sediments analyzed in Table 2. In all but one sediment off Africa, ratios were around 0.1–0.3, strongly indicating the preponderance of combustion processes for those samples. The $\Sigma Me\text{-phen/phen}$ ratio varied in the sediments off South America: in the Amazon fan, ratios were around 0.2, while ranging from 0.1 to 0.7 in samples from Brazil and Argentine (Table 2). The ratio of fluoranthene/(fluoranthene + pyrene) was above 0.5 for almost all samples, indicating that the combustion of grass, wood, and/or coal were responsible for the PAHs [Yunker *et al.*, 2002]. The highest ratios (~ 0.8) obtained were for the samples off Africa and the Amazon fan, with the other samples around 0.75 (Table 2). This further supports the conclusion that the majority of PAHs were combustion derived at all investigated sites. We were only able to determine the ratio of 1, 7- to 2, 6-dimethylphenanthrene for several sediment samples off the African coast, all yielding a ratio of close to 1. This would imply that vehicular traffic was more important ($\sim 2/3$) than wood burning as a source of the PAHs, and thus by inference also of the soot BC in the sediments [Benner *et al.*, 1995]. PAH ratios have been used frequently to apportion sources in coastal sediments [e.g., Yunker *et al.*, 2002], but the degree to which PAH ratios are conserved in deep sea sediments is unclear.

[35] Retene, an indicator of coniferous wood burning, was present at higher concentrations off Africa than South America (Table 2). It also displayed a significant positive correlation with latitude along the African coast ($r^2 = 0.87$), and a negative correlation with longitude across the South Atlantic ($r^2 = 0.43$), similar to total PAHs ($r^2 = 0.46$) (data not shown). This was in contrast to soot BC fluxes, which had a much weaker correlation with longitude ($r^2 = 0.31$). These results could suggest that soot BC was more persistent than PAHs, that the African sediments received additional PAHs from river discharges, or a combination of both.

[36] We had hypothesized that PAHs would be preferentially adsorbed to the soot BC, and thus give insights into its sources. $\Sigma PAHs$ correlated significantly with the sediment OC fraction ($r^2 = 0.62$) (Figure 3a), but only to a lesser degree with the soot BC fraction ($r^2 = 0.08$, Figure 3b). The difference between the transport of $\Sigma PAHs$ and soot BC was also evident in the settling fluxes (Table 2). Soot BC

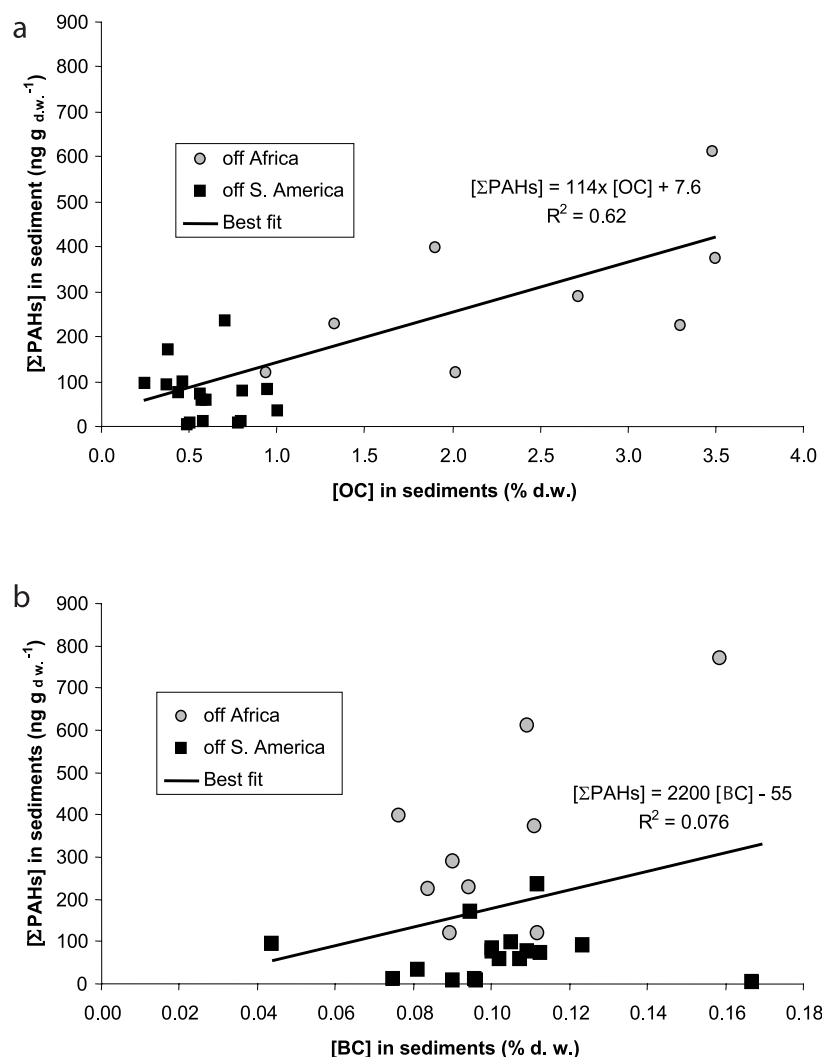


Figure 3. Σ PAHs concentration ($\text{ng g}^{-1} \text{dw}$) versus (a) OC and (b) soot BC concentrations (% dw) in South Atlantic sediments.

fluxes decreased on average two- to threefold from Africa to South America, whereas PAH fluxes decreased by five- to thirtyfold. This could be due to reactions rendering the soot BC's surface more hydrophilic which would tend to liberate the adsorbed PAHs [Czimeczik and Masiello, 2007] and reactions depleting the PAHs. Alternatively, the lack of PAH and soot BC correlation could be explained by the mixing of two or more different sources of soot BC with distinct PAH signatures each, such as additional riverine inputs off the African continent.

3.5. Estimation of Soot BC Deposition to the South Atlantic Based on Published Emission Estimates

[37] As has become apparent in the preceding discussion, there is very little measured data on soot BC fluxes in oceans. We therefore turned to atmospheric emission and deposition modeling for estimates of BC fluxes to the South Atlantic. Preliminary elementary carbon (EC) deposition data for the South Atlantic was obtained on the basis of model simulations performed with a coupled climate model

for the period of 1860–2000 [Stier *et al.*, 2006]. In the atmospheric community, EC is often measured by optical methods [e.g., Currie *et al.*, 2002]. Transient EC emission fluxes from 1860 to 2000 from fossil fuel combustion, domestic fuel wood consumption, agricultural waste burning, and forest fires are prescribed from a compilation by T. Nozawa *et al.* (NIES, personal communication, 2004). The global annual total aerosol and aerosol precursor emissions from 1860 to 2000 are dominated by forest fires and fossil fuel uses (Figure 4a).

[38] These results were derived from transient climate simulations produced for the International Panel on Climate Change (IPCC). In these simulations, wet deposition of EC to the ocean surface dominated over dry deposition. Historical deposition fluxes were summed to cover the same time period as accumulated in the sediments. EC flux estimates were higher off the African coast than off South America. Off Africa, simulated EC fluxes were highest off Cameroon ($7.5 \mu\text{g cm}^{-2} \text{a}^{-1}$), and approximately half that in the Congo fan ($3.3 \mu\text{g cm}^{-2} \text{a}^{-1}$). Off South America,

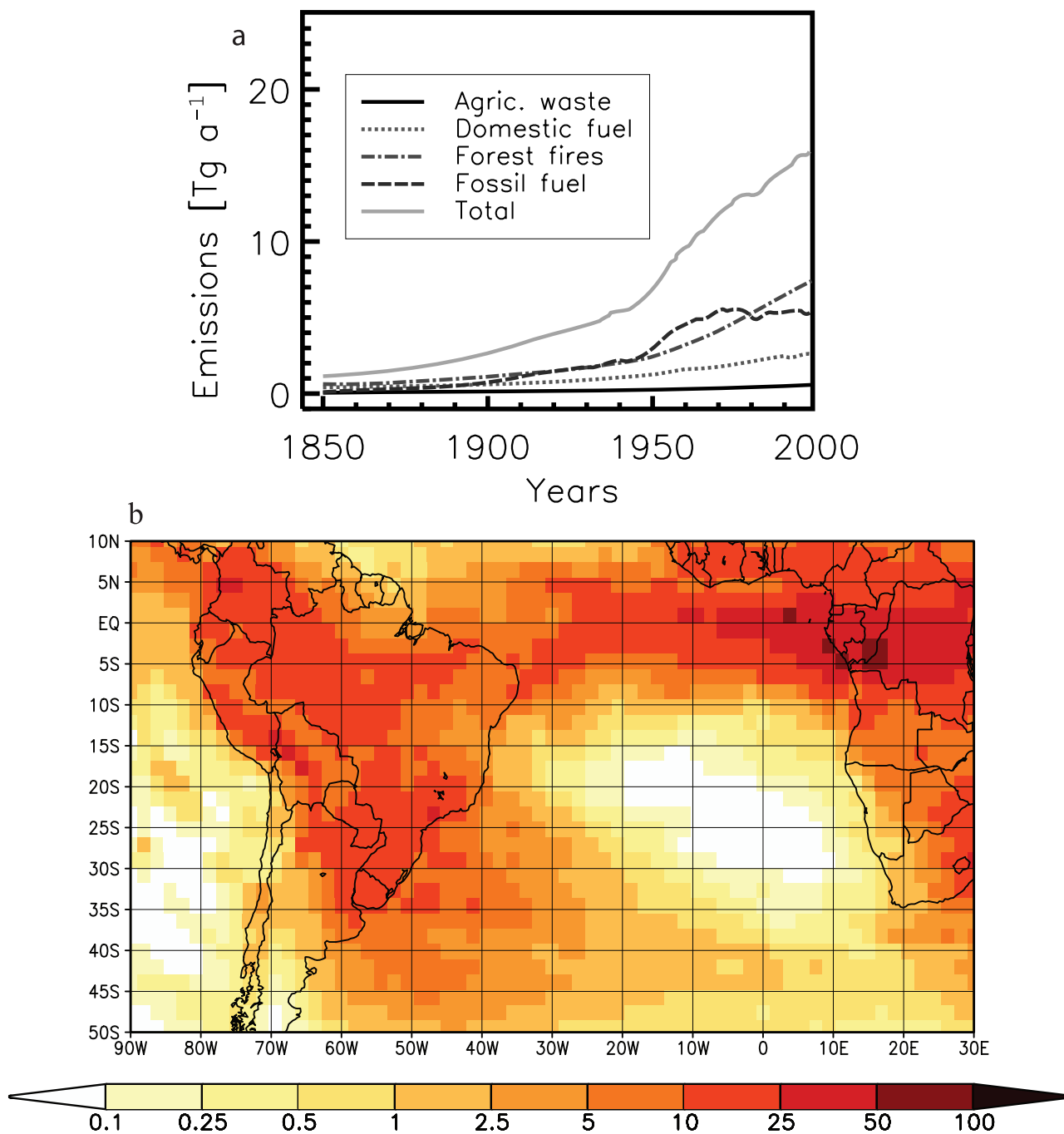


Figure 4. (a) Global annual source specific and total BC emissions from 1860 to 2000 in Tg C (T. Nozawa et al., NIES, personal communication, 2004). (b) Annual mean atmospheric EC deposition fluxes (sum of dry deposition, wet deposition, and sedimentation) as modeled for the year 1999 ($\mu\text{g cm}^{-2} \text{a}^{-1}$).

simulated EC fluxes were highest for the northern Brazil basin ($2.2 \mu\text{g cm}^{-2} \text{a}^{-1}$), and the Santos plateau ($1.6 \mu\text{g cm}^{-2} \text{a}^{-1}$), while simulated EC fluxes were around $0.6\text{--}0.8 \mu\text{g cm}^{-2} \text{a}^{-1}$ for the other regions.

[39] It is difficult to correctly convert EC fluxes to soot BC equivalents. Thermo-optical transmission (TOT) methods, which are commonly used to detect atmospheric EC, yielded 2–4 times higher results for urban aerosols than

method CTO-375 [Currie et al., 2002]. As both TOT and CTO-375 rely on a thermal distinction between OC and soot BC, we assume that a factor of 3 (2–4) can be used to convert the TOT results to soot BC measurements based on CTO-375, with an approximately twofold uncertainty. The atmospheric modeling results simulated average soot BC settling fluxes off Africa of $\sim 0.5\text{--}2 \mu\text{g cm}^{-2} \text{a}^{-1}$, and around $0.5\text{--}1 \mu\text{g cm}^{-2} \text{a}^{-1}$ off South America. The

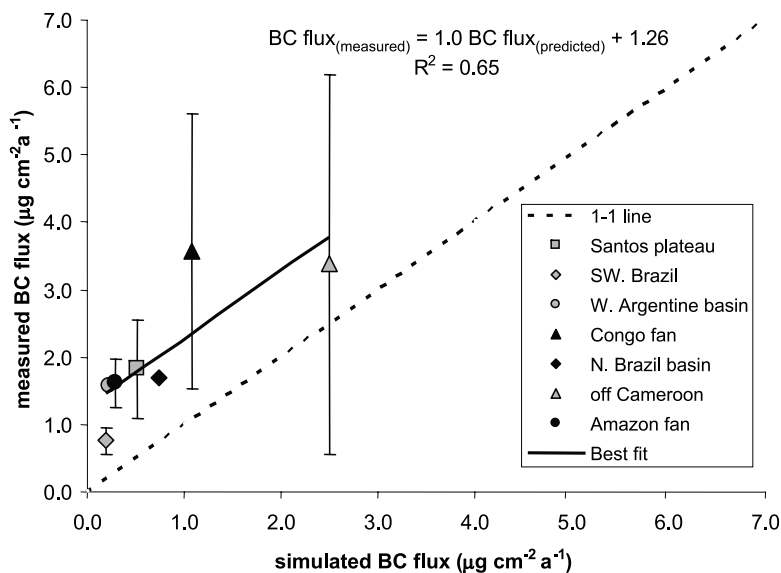


Figure 5. Measured versus simulated sedimentation fluxes of soot BC in South Atlantic sediments. Atmospheric BC deposition fluxes were simulated from a coupled aerosol-climate model using EC emission estimates for 1860–2000.

measured sedimentary soot BC fluxes exceed the simulated ones based on atmospheric deposition by factors of 2–5 (Figure 5). The simulated soot BC fluxes were solely based on atmospheric deposition. The atmospheric model could underestimate measured sedimentary soot BC fluxes due to additional riverine inputs, or if graphitic black carbon had contributed toward what we identified as soot BC [e.g., Dickens *et al.*, 2004a, 2004b]. Overestimations could result from soot BC being transformed to dissolved organic carbon (DOC) [e.g., Hockaday *et al.*, 2006]. Measured soot BC fluxes exceeded simulated fluxes on average 3.3 times in the Congo fan region, and 5.7 times in the Amazon fan region, potentially highlighting the importance of riverine soot BC delivery to the sediments. The Congo (Zaire) delivers ~ 48 Gg total suspended solids (TSS) a^{-1} . Soot BC constitutes on average 0.2% of TSS in rivers [Mitra *et al.*, 2002; Elmquist *et al.*, 2008]. If all soot BC was retained within the southwestern African regional province (see Table 3), an additional $2.4 \mu\text{g soot BC cm}^{-2} \text{a}^{-1}$ would be delivered. Discharge of soot BC from the

Congo would hence close the gap between simulated ($\sim 1.1 \mu\text{g cm}^{-2} \text{a}^{-1}$) and measured ($\sim 3.6 \mu\text{g cm}^{-2} \text{a}^{-1}$) soot BC fluxes. This is also inline with the observed terrestrial $\delta^{13}\text{C}$ signature of the OC in Congo River fan sediments (see above).

[40] Conversely, soot BC fluxes in sediments from the Amazon fan region ($\sim 1.6 \mu\text{g cm}^{-2} \text{a}^{-1}$) exceeded simulated atmospheric deposition ($0.3 \mu\text{g cm}^{-2} \text{a}^{-1}$) by $\sim 1 \mu\text{g cm}^{-2} \text{a}^{-1}$. If the total TSS discharge from the Amazon (~ 1.2 Pg TSS a^{-1}) was retained in the Brazilian continental margin, it would result in soot BC fluxes of $\sim 120 \mu\text{g cm}^{-2} \text{a}^{-1}$ (if BC constituted 0.2% of TSS). The fact that much less BC was detected in the Amazon fan could be due to the efficiency of the Amazon fan in remineralizing carbon [Aller and Blair, 2006].

[41] Similarly, measured sedimentary soot BC fluxes also exceeded simulated fluxes in regions outside of big river fans, such as the Argentine basin, Santos plateau and southwestern Brazil basin. Measured soot BC fluxes exceeded simulated fluxes by the largest margin (7 times)

Table 3. Regional Areas, Their Extent, Measured and Extrapolated Fluxes (Area Averaged) of Soot BC and PAHs, Flux of Particulate Organic Carbon (J_{POC}) and the Fraction J_{POC} Accounted for by Soot BC Fluxes

Regional Area	Areal Extent (km ²)	Measured Soot BC Flux ($\mu\text{g cm}^{-2} \text{a}^{-1}$)	Measured PAH Flux ($\text{ng cm}^{-2} \text{a}^{-1}$)	Extrapolated Soot BC Flux ^a (Gg a^{-1})	Extrapolated PAH Flux ^a (Mg a^{-1})	J_{POC} Flux (Gg a^{-1})	BC % of J_{POC}
SW African	1,915,460	3.5 ± 2.4	1.26 ± 1.10	66 ± 45	24 ± 21	10,000	0.7%
Argentinian continental margin	517,714	1.9 ± 0.6	0.23 ± 0.1	10 ± 3	1.2 ± 0.5	900	1.1%
Brazilian continental margin	1,045,260	1.4 ± 0.5	0.04 ± 0.03	15 ± 5	0.9 ± 1.0	1,900	0.8%
Central S Atlantic ^b	37,359,200	n/a	n/a	557	n/a	55,700	1% ^c
Total S Atlantic				~ 660	≥ 26		

^aExtrapolated fluxes are measured fluxes \times total area of the region.

^bHere n/a is not available.

^cAssumed value (see text).

in the western Argentine basin. For the Santos plateau and the southwestern Brazil basin, measured fluxes were ~ 4 times higher, while the agreement for the northern Brazil basin was within a factor of 2.3. Soot BC fluxes in samples off Cameroon and Libreville were close to simulations (1.4 times higher than simulated). Overall, the model simulated fluxes of soot BC reasonably well, higher fluxes off the African coast, lower fluxes off the South American coast. Measured soot BC fluxes exceed the model results in all cases by more than $1 \mu\text{g cm}^{-2} \text{ a}^{-1}$ on average. On the African side, riverine delivery of soot BC could account for the discrepancy, but not off South America. Additional work is needed to constrain the importance of rivers in delivering soot BC to South Atlantic sediments and the role of soot BC losses to the DOC pool.

[42] Results from the ECHAM model suggested that biomass burning plumes during the Southern Hemisphere's summer contributed most of the soot BC to the South Atlantic (Figure 4b). For present-day conditions, atmospheric BC deposition over the South Atlantic originates at low latitudes from vegetation fires and biofuel use in southern Africa and at midlatitudes from the Amazon region. The importance of natural fuels was only partially reflected in the PAH results, while both model results and measurements point toward combustion processes as the main emission sources (see above).

3.6. Budget Estimates of Soot BC Deposition to the South Atlantic

[43] Depositional fluxes of soot BC were computed for the different regional provinces from which sediments were analyzed (Table 3). The average soot BC flux was extrapolated to the entire provincial region [Seiter *et al.*, 2005], and compared to the regional flux of particulate organic carbon (J_{POC}). Highest soot BC fluxes were calculated for southwest Africa, at around 66 Gg a^{-1} , with another 10 and 15 Gg a^{-1} of soot BC deposited to the Argentinean and Brazilian continental margins, respectively. The soot BC fluxes to the sediments comprised around 1% of J_{POC} , from 0.7% off the African coast to 1.1% off the Argentinean coast (Table 3). The lower contribution of soot BC fluxes to J_{POC} were obtained for the high-productivity (and settling) areas off Africa and the Brazilian continental margin. No sediment samples from the interior of the South Atlantic were analyzed in this study. If we assumed that soot BC accounted for $\sim 0.7\text{--}1.1\%$ of J_{POC} , then the interior South Atlantic would bury an additional $390\text{--}610 \text{ Gg a}^{-1}$ soot BC. In total, we estimate that the South Atlantic buried around $480\text{--}700 \text{ Gg soot BC a}^{-1}$ in surface sediments below 1000 m water depth. This estimation of soot BC deposition excludes the region of highest simulated atmospheric deposition (south of equator, see Figure 4b). The export flux of soot BC in the South Atlantic is comparable in magnitude to an estimated flux of $400\text{--}800 \text{ Gg soot BC a}^{-1}$ to the continental shelf off New England [Gustafsson and Gschwend, 1998]. The predicted PAH burial flux for the South Atlantic is on the order of 26 Mg a^{-1} for the sample regions analyzed (Table 3). In contrast to soot BC, there is evidence that the majority of PAHs do not reach great depths [Bouloubassi *et al.*, 2006].

[44] The South Atlantic is estimated to receive a total discharge of $\sim 650,000 \text{ Gg TSS a}^{-1}$ from rivers [Ludwig and Probst, 1998], resulting in a soot BC flux delivery of $\sim 1,300 \text{ Gg a}^{-1}$ (if BC constituted 0.2% of TSS). These flux estimates suggest that for the South Atlantic, atmospheric deposition fluxes (including the equatorial deposition) might be as important as the riverine delivery of soot BC. Other studies imply the predominance of riverine soot BC delivery over atmospheric deposition [Mitra *et al.*, 2002; Elmquist *et al.*, 2008]. Elmquist *et al.* [2008] estimated that the Pan-Arctic rivers export 200 Gg BC a^{-1} , while Mitra *et al.* [2002] suggested fluxes of 500 Gg BC a^{-1} from the Mississippi. Elmquist *et al.* [2008] extrapolated these fluxes to the global scale and derived that the global soot BC flux from rivers ($\sim 26 \text{ Tg a}^{-1}$) was comparable to highest estimates of soot BC emissions (22 Tg a^{-1}). Riverine discharges could have been overestimated because of old BC being exported, or lower TSS fluxes [Elmquist *et al.*, 2008]. Our results imply that the atmospheric delivery of soot BC can play a significant role for an ocean basin, such as the South Atlantic. On the basis of global climate model runs, atmospheric deposition is also expected to be an important BC vector for the Indian Ocean. This suggests that attempts to construct a global mass balance of BC should include estimates of the atmospheric deposition of BC.

4. Conclusion and Outlook

[45] Our results imply that soot BC is refractory in deep sea sediments accounting for up to 35% of TOC. The bulk of soot BC is stored in the most remote sediments of the South Atlantic, in which we expect soot BC to contribute substantially to TOC. The $\delta^{13}\text{C}$ of soot BC measured in the South Atlantic were consistent with a major terrestrial carbon source. Analysis of PAHs and diagnostic ratios were used to characterize emission sources of the soot BC, suggesting the preponderance of combustion, particularly traffic emissions. In contrast, model results simulated BC emissions predominantly from forest fires and biomass burning. Future work should look at additional ways of attributing its sources.

[46] A reasonable agreement (factor of 2 to 4) was found between soot BC fluxes from an atmospheric model and measurements in the sediments. On the African side, riverine delivery of soot BC could have accounted for the discrepancy, but not off South America. Off Africa, higher PAH/soot BC ratios, higher concentrations of retene and the $\delta^{13}\text{C}$ values of the OC all supported additional, terrestrial carbon sources to the sediments. Additional effort is needed to constrain the importance of rivers in delivering soot BC to South Atlantic sediments and the role of soot BC losses to the DOC pool. Our results imply that the atmospheric delivery of soot BC can play a significant role for an ocean basin, such as the South Atlantic. Ideally, future work should aim to also measure these fluxes in other ocean basins, in the sediments, water column and atmosphere.

[47] **Acknowledgments.** R. Lohmann acknowledges support by the URI Council for Research for this research project, support by the Vetlesen and Monel foundations, K. Seiter (University of Bremen) for helpful discussion, A. Sweetman (Lancaster University) for producing Figure 2,

J. Sullivan (URI) for additional BC analyses, and two anonymous reviewers for their constructive comments.

References

- Aller, R. C., and N. E. Blair (2006), Carbon remineralization in the Amazon-Guianas tropical mobile mudbelt: A sedimentary incinerator, *Cont. Shelf Res.*, 26, 2241–2259, doi:10.1016/j.csr.2006.07.016.
- Benner, B. A., S. A. Wise, L. A. Currie, G. A. Klouda, D. B. Klinedinst, R. B. Zweidinger, R. K. Stevens, and C. W. Lewis (1995), Distinguishing the contributions of residential wood combustion and mobile source emissions using relative concentrations of dimethylphenanthrene isomers, *Environ. Sci. Technol.*, 29, 2382–2389, doi:10.1021/es00009a034.
- Bird, M. I., and J. A. Cali (1998), A million-year record of fire in sub-Saharan Africa, *Nature*, 394, 767–769, doi:10.1038/29507.
- Bird, M. I., C. Moyo, E. M. Veenendaal, J. Lloyd, and P. Frost (1999), Stability of elemental carbon in a savanna soil, *Global Biogeochem. Cycles*, 13, 923–932, doi:10.1029/1999GB900067.
- Blumer, M. (1976), Polycyclic aromatic hydrocarbons in nature, *Sci. Am.*, 3, 35–45.
- Bond, T. C., D. G. Streets, K. F. Yarber, S. M. Nelson, J. H. Woo, and Z. Klimont (2004), A technology-based global inventory of black and organic carbon emissions from combustion, *J. Geophys. Res.*, 109, D14203, doi:10.1029/2003JD003697.
- Bouloubassi, I., L. Méjanelle, R. Pete, J. Fillaux, A. Lorre, and V. Point (2006), PAH transport by sinking particles in the open Mediterranean Sea: A 1 year sediment trap study, *Mar. Pollut. Bull.*, 52, 560–571, doi:10.1016/j.marpolbul.2005.10.003.
- Buckley, D. R., K. J. Rockne, A. Li, and W. J. Mills (2004), Soot deposition in the Great Lakes: Implications for semi-volatile hydrophobic organic pollutant deposition, *Environ. Sci. Technol.*, 38, 1732–1739, doi:10.1021/es034926t.
- Burdige, D. J. (2005), Burial of terrestrial organic matter in marine sediments: A re-assessment, *Global Biogeochem. Cycles*, 19, GB4011, doi:10.1029/2004GB002368.
- Cachier, H. (1989), Isotopic characterization of carbonaceous aerosols, *Aerosol Sci. Technol.*, 10, 379–385, doi:10.1080/02786828908959276.
- Cooke, W. F., C. Lioussse, H. Cachier, and J. Feichter (1999), Construction of a $1^\circ \times 1^\circ$ fossil fuel emission data set for carbonaceous aerosol and implementation and radiative impact in the ECHAM4 model, *J. Geophys. Res.*, 104, 22,137–22,162.
- Cooke, W. F., V. Ramaswamy, and P. Kasibhatla (2002), A general circulation model study of the global carbonaceous aerosol distribution, *J. Geophys. Res.*, 107(D16), 4279, doi:10.1029/2001JD001274.
- Cornelissen, G., O. Gustafsson, T. D. Bucheli, M. T. O. Jonker, A. A. Koelmans, and P. C. M. Van Noort (2005), Extensive sorption of organic compounds to black carbon, coal, and kerogen in sediments and soils: Mechanisms and consequences for distribution, bioaccumulation, and biodegradation, *Environ. Sci. Technol.*, 39, 6881–6895, doi:10.1021/es050191b.
- Crutzen, P. J., and M. O. Andreae (1990), Biomass burning in the tropics: Impact on atmospheric chemistry and biogeochemical cycles, *Science*, 250, 1669–1678, doi:10.1126/science.250.4988.1669.
- Currie, L. A., G. A. Klouda, B. A. Benner, K. Garrity, and T. I. Eglinton (1999), Isotopic and molecular fractionation in combustion; three routes to molecular marker validation, including direct molecular “dating” (GC/AMS), *Atmos. Environ.*, 33, 2789–2806, doi:10.1016/S1352-2310(98)00325-2.
- Currie, L. A., et al. (2002), A critical evaluation of interlaboratory data on total, elemental, and isotopic carbon in the carbonaceous particle reference material, NIST SRM 1649a, *J. Res. Natl. Inst. Stand. Technol.*, 107, 279–298.
- Czimeczik, C. I., and C. A. Masiello (2007), Controls on black carbon storage in soils, *Global Biogeochem. Cycles*, 21, GB3005, doi:10.1029/2006GB002798.
- Dachs, J., and S. J. Eisenreich (2000), Adsorption onto aerosol soot carbon dominates gas-particle partitioning of polycyclic aromatic hydrocarbons, *Environ. Sci. Technol.*, 34, 3690–3697, doi:10.1021/es991201+.
- Dickens, A. F., Y. Gelin, and J. I. Hedges (2004a), Physical separation of combustion and rock sources of graphitic black carbon in sediments, *Mar. Chem.*, 92, 215–223, doi:10.1016/j.marchem.2004.06.027.
- Dickens, A. F., Y. Gelin, C. A. Masiello, S. Wakeham, and J. I. Hedges (2004b), Reburial of fossil organic carbon in marine sediments, *Nature*, 427, 336–339, doi:10.1038/nature02299.
- Eglinton, T. I., G. Eglinton, L. Dupont, E. R. Sholkovitz, D. Montlucon, and C. M. Reddy (2002), Composition, age, and provenance of organic matter in NW African dust over the Atlantic Ocean, *Geochem. Geophys. Geosyst.*, 3(8), 1050, doi:10.1029/2001GC000269.
- Elmquist, M., O. Gustafsson, and P. Andersson (2004), Quantification of sedimentary black carbon using the chemothermal oxidation method: An evaluation of ex situ pretreatments and standard additions approaches, *Limnol. Oceanogr. Methods*, 2, 417–427.
- Elmquist, M., G. Cornelissen, Z. Kukulska, and O. Gustafsson (2006), Distinct Oxidative stabilities of char versus soot black carbon: Implications for quantification and environmental recalcitrance, *Global Biogeochem. Cycles*, 20, GB2009, doi:10.1029/2005GB002629.
- Elmquist, M., Z. Zencak, and O. Gustafsson (2007), A 700 year sediment record of black carbon and polycyclic aromatic hydrocarbons near the EMEP air monitoring station in Aspövret, Sweden, *Environ. Sci. Technol.*, 41, 6926–6932, doi:10.1021/es070546m.
- Elmquist, M., I. Semiletov, L. D. Guo, and O. Gustafsson (2008), Pan-Arctic patterns in black carbon sources and fluvial discharges deduced from radiocarbon and PAH source apportionment markers in estuarine surface sediments, *Global Biogeochem. Cycles*, 22, GB2018, doi:10.1029/2007GB002994.
- Farquhar, G. D., J. R. Ehleringer, and K. T. Hubick (1989), Carbon isotope discrimination and photosynthesis, *Annu. Rev. Plant Physiol. Plant Mol. Biol.*, 40, 503–537, doi:10.1146/annurev.pp.40.060189.002443.
- Gelin, Y., K. M. Prentice, J. A. Baldock, and J. I. Hedges (2001), An improved thermal oxidation method for the quantification of soot/graphitic black carbon in sediments and soils, *Environ. Sci. Technol.*, 35, 3519–3525, doi:10.1021/es010504c.
- Goldberg, E. D. (1985), *Black Carbon in the Environment*, Wiley, New York.
- Gustafsson, O., and P. M. Gschwend (1997), Soot as a strong partition medium for polycyclic aromatic hydrocarbons in aquatic systems, in *Molecular Markers in Environmental Geochemistry*, edited by R. P. Eganhouse, pp. 365–381, Am. Chem. Soc., Washington, D. C.
- Gustafsson, O., and P. M. Gschwend (1998), The flux of black carbon to surface sediments on the New England continental shelf, *Geochim. Cosmochim. Acta*, 62, 465–472, doi:10.1016/S0016-7037(97)00370-0.
- Gustafsson, O., F. Haghseta, C. Chan, J. MacFarlane, and P. M. Gschwend (1997), Quantification of the dilute sedimentary soot phase: Implications for PAH speciation and bioavailability, *Environ. Sci. Technol.*, 31, 203–209, doi:10.1021/es960317s.
- Gustafsson, O., T. D. Bucheli, Z. Kukulska, M. Andersson, C. Largeau, J. N. Rouzaud, C. M. Reddy, and T. I. Eglinton (2001), Evaluation of a protocol for the quantification of black carbon in sediments, *Global Biogeochem. Cycles*, 15, 881–890, doi:10.1029/2000GB001380.
- Hammes, K., et al. (2007), Comparison of quantification methods to measure fire-derived (black/elemental) carbon in soils and sediments using reference materials from soil, water, sediment and the atmosphere, *Global Biogeochem. Cycles*, 21, GB3016, doi:10.1029/2006GB002914.
- Hansen, J., et al. (2005), Efficacy of climate forcings, *J. Geophys. Res.*, 110, D18104, doi:10.1029/2005JD005776.
- Hartmann, P. C., J. G. Quinn, R. W. Cairns, and J. W. King (2004), The distribution and sources of polycyclic aromatic hydrocarbons in Narragansett Bay surface sediments, *Mar. Pollut. Bull.*, 48, 351–358, doi:10.1016/j.marpolbul.2003.08.014.
- Hartnett, H. E., R. G. Keil, J. I. Hedges, and A. H. Devol (1998), Influence of oxygen exposure time on organic carbon preservation in continental margin sediments, *Nature*, 391, 572–574, doi:10.1038/35351.
- Hockaday, W. C., A. M. Grannas, S. Kim, and P. G. Hatcher (2006), Direct molecular evidence for the degradation and mobility of black carbon in soils from ultrahigh-resolution mass spectral analysis of dissolved organic matter from a fire-impacted forest soil, *Org. Geochem.*, 37, 501–510, doi:10.1016/j.orggeochem.2005.11.003.
- Holtvoeth, J., T. Wagner, and C. J. Schubert (2003), Organic matter in river-influenced continental margin sediments: The land-ocean and climate linkage at the Late Quaternary Congo fan (ODP Site 1075), *Geochem. Geophys. Geosyst.*, 4(12), 1109, doi:10.1029/2003GC000590.
- Ito, A., and J. E. Penner (2005), Historical emissions of carbonaceous aerosols from biomass and fossil fuel burning for the period 1870–2000, *Global Biogeochem. Cycles*, 19, GB2028, doi:10.1029/2004GB002374.
- Jaward, F. M., J. L. Barber, K. Booij, and K. C. Jones (2004), Spatial distribution of atmospheric PAHs and PCNs along a north-south Atlantic transect, *Environ. Pollut.*, 132, 173–181, doi:10.1016/j.envpol.2004.03.029.
- Jenk, T. M., S. Szidat, M. Schwikowski, H. W. Gaggeler, S. Brutsch, L. Wacker, H. A. Sinal, and M. Saurer (2006), Radiocarbon analysis in an Alpine ice core: Record of anthropogenic and biogenic contributions to carbonaceous aerosols in the past (1650–1940), *Atmos. Chem. Phys.*, 6, 5381–5390.
- Kinne, S., et al. (2003), Monthly averages of aerosol properties: A global comparison among models, satellite data, and AERONET

- ground data, *J. Geophys. Res.*, *108*(D20), 4634, doi:10.1029/2001JD001253.
- Kuhlbusch, T. A. J. (1998), Black carbon and the carbon cycle, *Science*, *280*, 1903–1904, doi:10.1126/science.280.5371.1903.
- Kuhlbusch, T. A. J., and P. J. Crutzen (1995), Toward a global estimate of black carbon in residues of vegetation fires representing a sink of atmospheric CO₂ and a source of O₂, *Global Biogeochem. Cycles*, *9*, 491–501, doi:10.1029/95GB02742.
- Lavanchy, V. M. H., H. W. Gaggeler, U. Schotterer, M. Schwikowski, and U. Baltensperger (1999), Historical record of carbonaceous particle concentrations from a European high-alpine glacier (Colle Gnifetti, Switzerland), *J. Geophys. Res.*, *104*, 21,227–21,236.
- Lohmann, R., and G. Lammel (2004), Adsorptive and absorptive contributions to the gas-particle partitioning of polycyclic aromatic hydrocarbons: State of knowledge and recommended parameterization for modeling, *Environ. Sci. Technol.*, *38*, 3793–3803, doi:10.1021/es035337q.
- Lohmann, R., J. K. MacFarlane, and P. M. Gschwend (2005), Importance of black carbon to sorption of native PAHs, PCBs, and PCDDs in Boston and New York Harbor sediments, *Environ. Sci. Technol.*, *39*, 141–148, doi:10.1021/es049424+.
- Louchouart, P., S. N. Chillrud, S. Houel, B. Yan, D. Chaky, C. Rumpel, C. Largeau, G. Bardoux, D. Walsh, and R. F. Bopp (2007), Elemental and molecular evidence of soot- and char-derived black carbon inputs to New York City's atmosphere during the 20th century, *Environ. Sci. Technol.*, *41*, 82–87, doi:10.1021/es061304+.
- Ludwig, W., and J. L. Probst (1998), River sediment discharge to the oceans: Present-day controls and global budgets, *Am. J. Sci.*, *298*, 265–295.
- Mannino, A., and H. R. Harvey (2004), Black carbon in estuarine and coastal ocean dissolved organic matter, *Limnol. Oceanogr.*, *49*, 735–740.
- Middelburg, J. J., K. Soetaert, and P. M. J. Herman (1997), Empirical relationships for use in global diagenetic models, *Deep Sea Res. Part I*, *44*, 327–344, doi:10.1016/S0967-0637(96)00101-X.
- Middelburg, J. J., J. Nieuwenhuize, and P. van Breugel (1999), Black carbon in marine sediments, *Mar. Chem.*, *65*, 245–252, doi:10.1016/S0304-4203(99)00005-5.
- Mitra, S., T. S. Bianchi, B. A. McKee, and M. Sutula (2002), Black carbon from the Mississippi River: Quantities, sources, and potential implications for the global carbon cycle, *Environ. Sci. Technol.*, *36*, 2296–2302, doi:10.1021/es015834b.
- Nguyen, T. H., R. A. Brown, and W. P. Ball (2004), An evaluation of thermal resistance as a measure of black carbon content in diesel soot, wood char, and sediment, *Org. Geochem.*, *35*, 217–234, doi:10.1016/j.orggeochem.2003.09.005.
- Nizzetto, L., R. Lohmann, R. Gioia, A. Jahnke, C. Temme, J. Dachs, P. Herckes, A. Di Guardo, and K. C. Jones (2008), PAHs in air and seawater along a North-South Atlantic transect: Trends, processes and possible sources, *Environ. Sci. Technol.*, *42*, 1580–1585, doi:10.1021/es0717414.
- Ohkouchi, N., K. Kawamura, and H. Kawahata (1999), Distributions of three- to seven-ring polycyclic aromatic hydrocarbons on the deep sea floor in the central Pacific, *Environ. Sci. Technol.*, *33*, 3086–3090, doi:10.1021/es981181w.
- Roeckner, E., et al. (2003), *The Atmospheric General Circulation Model ECHAM5. Part I: Model Description*, Max Planck Inst. for Meteorol., Hamburg, Germany.
- Sato, M., J. Hansen, D. Koch, A. Lacis, R. Ruedy, O. Dubovik, B. Holben, M. Chin, and T. Novakov (2003), Global atmospheric black carbon inferred from AERONET, *Proc. Natl. Acad. Sci. U. S. A.*, *100*, 6319–6324, doi:10.1073/pnas.0731897100.
- Schaap, M., H. Van Der Gon, F. J. Dentener, A. J. H. Visschedijk, M. Van Loon, H. M. ten Brink, J. P. Putaud, B. Guillaume, C. Lioussé, and P. J. H. Buitjes (2004), Anthropogenic black carbon and fine aerosol distribution over Europe, *J. Geophys. Res.*, *109*, D18207, doi:10.1029/2003JD004330.
- Schmidt, M. W. I., and A. G. Noack (2000), Black carbon in soils and sediments: Analysis, distribution, implications, and current challenges, *Global Biogeochem. Cycles*, *14*, 777–793, doi:10.1029/1999GB001208.
- Schmidt, M. W. I., J. O. Skjemstad, and C. Jaeger (2002), Carbon isotope geochemistry and nanomorphology of soil black carbon: Black chernozemic soils in central Europe originate from ancient biomass burning, *Global Biogeochem. Cycles*, *16*(4), 1123, doi:10.1029/2002GB001939.
- Schult, I., J. Feichter, and W. F. Cooke (1997), Effect of black carbon and sulfate aerosols on the Global Radiation Budget, *J. Geophys. Res.*, *102*, 30,107–30,117.
- Seiler, W., and P. J. Crutzen (1980), Estimates of gross and net fluxes of carbon between the biosphere and the atmosphere from biomass burning, *Clim. Change*, *2*, 207–247, doi:10.1007/BF00137988.
- Seiter, K., C. Hensen, and M. Zabel (2005), Benthic carbon mineralization on a global scale, *Global Biogeochem. Cycles*, *19*, GB1010, doi:10.1029/2004GB002225.
- Smith, D. M., J. J. Griffin, and E. D. Goldberg (1973), Elemental carbon in marine sediments: A baseline for burning, *Nature*, *241*, 268–270, doi:10.1038/241268a0.
- Stier, P., et al. (2005), The aerosol-climate model ECHAM5-HAM, *Atmos. Chem. Phys.*, *5*, 1125–1156.
- Stier, P., J. Feichter, E. Roeckner, S. Kloster, and M. Esch (2006), The evolution of the global aerosol system in a transient climate simulation from 1860 to 2100, *Atmos. Chem. Phys.*, *6*, 3059–3076.
- Takemura, T., T. Nozawa, S. Emori, T. Y. Nakajima, and T. Nakajima (2005), Simulation of climate response to aerosol direct and indirect effects with aerosol transport-radiation model, *J. Geophys. Res.*, *110*, D02202, doi:10.1029/2004JD005029.
- Vignati, E., J. Wilson, and P. Stier (2004), M7: An efficient size-resolved aerosol microphysics module for large-scale aerosol transport models, *J. Geophys. Res.*, *109*, D22202, doi:10.1029/2003JD004485.
- Wagner, T., M. Zabel, L. Dupont, J. Holtvoeth, and C. J. Schubert (2003), Terrigenous signal in sediments of the low latitude Atlantic—Implication for environmental variations during the late Quaternary, part I: Organic carbon, in *The South Atlantic in the Late Quaternary: Reconstruction of Material Budgets and Current Systems*, edited by G. Wefer, S. Mulitza, and V. Ratmeyer, pp. 295–322, Springer, Berlin.
- Yunker, M. B., R. W. Macdonald, R. Vingarzan, R. H. Mitchell, D. Goyette, and S. Sylvestre (2002), PAHs in the Fraser River basin: A critical appraisal of PAH ratios as indicators of PAH source and composition, *Org. Geochem.*, *33*, 489–515, doi:10.1016/S0146-6380(02)00002-5.
- Zabel, M., T. Wagner, and P. deMenocal (2003), Terrigenous signals in sediments of the low-latitude Atlantic—Indications to environmental variations during the late Quaternary, part II: Lithogenic matter, in *The South Atlantic in the Late Quaternary: Reconstruction of Material Budgets and Current Systems*, edited by G. Wefer, S. Mulitza, and V. Ratmeyer, pp. 323–345, Springer, Berlin.
- K. Bollinger and R. Lohmann, Graduate School of Oceanography, University of Rhode Island, 215 South Ferry Road, Narragansett, RI 02882, USA. (lohmann@gso.uri.edu)
- M. Cantwell, ORD/NHEERL-Atlantic Ecology Division, U.S. Environmental Protection Agency, 27 Tarzwell Drive, Narragansett, RI 02882, USA.
- J. Feichter and I. Fischer-Bruns, Max Planck Institute for Meteorology, Bundesstraße 53, D-20146 Hamburg, Germany.
- M. Zabel, MARUM Geowissenschaften, University of Bremen, D-28334 Bremen, Germany.